

Age of Information in Federated Learning over Wireless Networks

Kaidi Wang, *Member, IEEE*, Yi Ma, *Senior Member, IEEE*, Mahdi Boloursaz Mashhadi, *Member, IEEE*, Chuan Heng Foh, *Senior Member, IEEE*, Rahim Tafazolli, *Senior Member, IEEE*, and Zhi Ding, *Fellow, IEEE*

Abstract—In this paper, federated learning (FL) over wireless networks is investigated. In each communication round, a subset of devices is selected to participate in the aggregation with limited time and energy. In order to minimize the convergence time, global loss and latency are jointly considered in a Stackelberg game based framework. Specifically, age of information (AoI) based device selection is considered at leader-level as a global loss minimization problem, while sub-channel assignment, computational resource allocation, and power allocation are considered at follower-level as a latency minimization problem. By dividing the follower-level problem into two sub-problems, the best response of the follower is obtained by a monotonic optimization based resource allocation algorithm and a matching based sub-channel assignment algorithm. By deriving the upper bound of convergence rate, the leader-level problem is reformulated, and then a list based device selection algorithm is proposed to achieve Stackelberg equilibrium. Simulation results indicate that the proposed device selection scheme outperforms other schemes in terms of the global loss, and the developed algorithms can significantly decrease the time consumption of computation and communication.

Index Terms—Age of information, device selection, federated learning (FL), resource allocation, sub-channel assignment

I. INTRODUCTION

With the rapid development of mobile devices and applications, the amount of data is exploded in the fifth-generation (5G) era, which leads to the great progress in machine learning (ML) [1]. In conventional centralized ML, a central server is equipped at the access point (AP) to collect all raw data for model training. However, due to the limited wireless resources and potential privacy issues, centralized ML is impractical for some scenarios [2]. In this context, federated learning (FL) has been proposed as a distributed ML algorithm to train neural networks while keeping the data locally [3]. Specifically, in FL, a global model is shared among multiple devices, and each device trains the received global model based on the local data and produces a local model [4]. After that, all local models are transmitted to the server via wireless communication networks to generate the updated global model [5]. Since the raw data does not leave the device, and the size of the model is much smaller than the data, privacy-sensitive issues can be avoided and less communication resources are consumed.

K. Wang, Y. Ma, M. Boloursaz Mashhadi, C. Foh, and R. Tafazolli are with 5GIC & 6GIC, Institute for Communication Systems (ICS), University of Surrey, Guildford, United Kingdom (email: kaidi.wang@ieee.org; y.ma@surrey.ac.uk; m.boloursazmashhadi@surrey.ac.uk; c.foh@surrey.ac.uk; r.tafazolli@surrey.ac.uk).

Z. Ding is with the Department of Electrical and Computer Engineering, University of California at Davis, Davis, CA 95616 USA (email: zding@ucdavis.edu).

A. Related Works

Due to the characteristics of FL, the related design and optimization in existing wireless communication architectures have attracted much attention. The convergence time, which is jointly determined by the number of communication rounds and the time consumption per round, is regarded as an important metric for evaluating the performance of FL [6].

By confirming the relationship between global loss and convergence bound, some works focused on the global loss minimization problem in order to increase the convergence rate, or reduce the number of required communication rounds [7]–[11]. Specifically, in [7], the authors have designed a FL algorithm with multiple local training. The impact of local and global update rounds on the convergence bound was analyzed, and the approximate solution of the global loss minimization problem was obtained. In [8], the packet error rate was introduced to indicate whether the parameter transmission was successful or not, and then user selection, resource block allocation, and power allocation were jointly studied under delay and energy constraints. FL was also considered in a massive multiple-input-multiple-output (MIMO) scenario with energy harvesting, where user scheduling and power allocation were included in the global loss minimization problem [9]. Moreover, this work was extended to a multi-cell system, and user association between users and base stations (BSs) was considered. The model pruning scheme was adopted in [10], where the unimportant weights can be set to zero in order to reduce the model size. In this paper, device selection, time slot allocation and pruning ratio were jointly optimized to maximize the convergence rate with a latency constraint. In [11], a global loss minimization problem was formulated with the total time consumption limitation, and then decoupled into a device scheduling problem and a bandwidth allocation problem. By analyzing the convergence bound of FL, the trade-off between the latency of each round and the number of required rounds was revealed.

As another factor in determining the convergence time, latency of FL, including computation time and communication time, was extensively researched in previous works [12]–[15]. In [12], a realistic wireless network was designed for FL, where a limited number of users can be selected at each round for aggregation. By obtaining user selection and resource block allocation schemes, the convergence time of FL was minimized. By setting a local accuracy level at each device, the FL algorithm with multiple local update rounds was proposed in a cell-free massive MIMO scenario

[13]. Moreover, in the formulated training time minimization problem, time consumption for downlink transmission, uplink transmission, and computation were comprehensively considered. A multi-task FL framework was studied in a multiaccess edge computing (MEC) scenario, where edge nodes were included to accomplish different learning tasks [14]. In order to minimize the latency of each communication round, the optimal matching between edge nodes and end devices was obtained. The authors in [15] have proposed a hybrid learning scheme which combined edge computing and FL. Particularly, part of data can be offloaded from devices to the server for training, and then the local models can be trained based on the remaining data. It was demonstrated that the proposed scheme has the ability to reduce the total time consumption.

B. Motivation and Contribution

As forwarded mentioned, global loss minimization and latency minimization were extensively researched in existing works. However, most works have studied it individually. As pointed out in [11], there exists a trade-off between global loss and latency. That is, some devices with the great positive impact on global loss may have poor channel conditions or weak computational capacities, and hence, the latency of this communication round will be obviously increased. Normally, the latency can be reduced by increasing transmit power or central processing unit (CPU) frequency, which means consuming more energy [16]. Hence, there exists another trade-off in FL, i.e., the interaction between latency and energy consumption. Even though global loss and latency were jointly studied in [11], it is necessary to consider the practical energy budget in a latency minimization problem and the possible impact on the global loss. In this paper, based on Stackelberg game, the interaction between global loss minimization and latency minimization are investigated with limited energy and time. It is revealed that the negative effects caused by energy and time constraints can be reduced by optimizing the CPU frequency and transmit power. On the other hand, due to the fact that the number of devices participating in FL is usually much larger than the number of available sub-channels, device selection is commonly considered in the FL based wireless communication framework. The conventional device selection scheme depends on either wireless resources [8] or local models [10], [12]. In this paper, a novel age of information (AoI) based device selection scheme is proposed, which can improve the convergence rate without analyzing local models. The main contributions are listed as follows:

- A latency-sensitive FL scenario is considered, where multiple devices transmit parameters to the server with the limited number of sub-channels. By introducing AoI, a weighed device selection scheme is proposed. In order to jointly minimize global loss and latency, a Stackelberg game based problem is formulated, where global loss minimization and latency minimization are considered as leader-level and follower-level problems, respectively.
- The follower-level problem is divided into two sub-problems, including resource allocation and sub-channel assignment. Due to non-convexity and monotonicity, a

monotonic optimization based solution is proposed for the resource allocation problem. Moreover, a matching based algorithm is developed to address the sub-channel assignment problem, where the properties of the proposed algorithm are analyzed.

- For solving the leader-level problem, the upper bound of the convergence rate is derived, and then the global loss minimization problem is reformulated as a weighted device selection problem. By ordering devices based on information age and data size, a list is established, and an algorithm is proposed to select devices by testing sub-channel assignment and resource allocation.
- The simulation results based on the Modified National Institute of Standards and Technology (MNIST) database is presented. It is indicated that the AoI based device selection algorithm can improve the performance of FL on both independent identically distributed (IID) and non-IID data. Moreover, the proposed solution of resource allocation can significantly reduce the latency of each communication round.

C. Organization

The remainder of this paper is organized as follows. In Section II and Section III, the system model and problem formulation are described, respectively. The solution of latency minimization problem is presented in Section IV, and the solution of global loss minimization problem is obtained in Section V. Section VI demonstrates the simulation results. The conclusions are summarized in Section VII.

II. SYSTEM MODEL

Consider an FL scenario where N wireless devices collaboratively train a joint learning model. Each device is equipped with a single antenna and the FL process is orchestrated by a wireless server. The set of all devices is denoted by $\mathcal{N} = \{1, 2, \dots, N\}$. Specifically, each device intends to train neural networks based on its local data and then transmit the parameters to the server for aggregation. The limited communication resources are considered in this paper. That is, there are K available sub-channels, where $K \leq N$, and each sub-channel can be occupied by one device. The set of all sub-channels is denoted by $\mathcal{K} = \{1, 2, \dots, K\}$. Therefore, in any round t , only a subset of devices can be selected for the global model aggregation. The procedure of the considered FL framework is presented as follows:

- 1) In any round t , the server broadcasts the global model $\mathbf{g}^{(t)}$ to all devices.
- 2) Each selected device trains the received global model and generate a local model $\mathbf{w}_n^{(t)}$.
- 3) The selected devices transmit local models to the server through the assigned sub-channels.
- 4) The server aggregates the received models to generate an updated global model $\mathbf{g}^{(t+1)}$.

Starting from $t = 1$, the above procedure will repeat until the FL converges.

A. Computation Model

After receiving the global model, the selected devices need to train their respective local learning models by utilizing the equipped CPUs. For any device n assigned to sub-channel k , the computational time consumption is given by

$$T_{k,n}^{\text{cp}}(\tau_{k,n}) = \frac{\mu\beta_n}{\tau_{k,n}C_n}, \quad (1)$$

where μ is a coefficient to denote the required CPU cycles for training one sample, β_n is the number of samples at device n , $\tau_{k,n}$ is a designed proportion of computational capacity, and C_n is the CPU frequency of device n . It is worth mentioning that the computation phase is affected by the assigned sub-channel, though without explicit channel gain in (1). Specifically, for any device, the time consumption and energy consumption of transmission vary with different sub-channels, and hence, the computational resource allocation coefficient τ should be dynamically adjusted according to allocated sub-channel gains. According to [17], the energy consumption for computation can be expressed as follows:

$$E_{k,n}^{\text{cp}}(\tau_{k,n}) = \kappa_0\mu\beta_n(\tau_{k,n}C_n)^2, \quad (2)$$

where κ_0 is the power consumption coefficient per CPU cycle.

B. Communication Model

At this phase, the local models are transmitted from the selected devices to the server. For any device n , the achievable data rate at sub-channel k is given by

$$R_{k,n}(P_{k,n}) = B \log_2(1 + P_{k,n}|h_{k,n}|^2), \quad (3)$$

where B is the bandwidth, $P_{k,n}$ is the transmit power of device n , and $|h_{k,n}|^2$ is the normalized channel gain. Particularly, $|h_{k,n}|^2 = |\tilde{h}_{k,n}|^2\sigma^{-2}$, where $\tilde{h}_{k,n}$ is the complex-value Gaussian channel between device n and the server via sub-channel k , and σ^2 is the variance of additive white Gaussian noise (AWGN). Based on the achievable data rate, the time consumption for communication can be presented as follows:

$$T_{k,n}^{\text{cm}}(P_{k,n}) = \frac{D(\mathbf{w}_n)}{R_{k,n}(P_{k,n})}, \quad (4)$$

where $D(\mathbf{w}_n)$ is the size of the local model at device n . It is assumed that the data size of local models is the same for all devices, i.e., $D(\mathbf{w}) = D(\mathbf{w}_n), \forall n \in \mathcal{N}$. The energy consumption for communication is given by

$$E_{k,n}^{\text{cm}}(P_{k,n}) = P_{k,n}T_{k,n}^{\text{cm}}(P_{k,n}). \quad (5)$$

C. Device Selection

Since the number of sub-channels is less than or equal to the number of devices, a subset of devices, denoted by \mathcal{N}_t , is selected in round t , i.e., $\mathcal{N}_t \subseteq \mathcal{N}$ and $|\mathcal{N}_t| \leq K$. The status of any device in round t can be represented by a binary variable $S_n^{(t)} \in \{0, 1\}$, where $S_n^{(t)} = 1$ indicates device n is selected to participate in the aggregation in round t ; $S_n^{(t)} = 0$ otherwise. The set of all device selection indicators is denoted by \mathbf{S} . Therefore, in any round, the set of selected devices \mathcal{N}_t

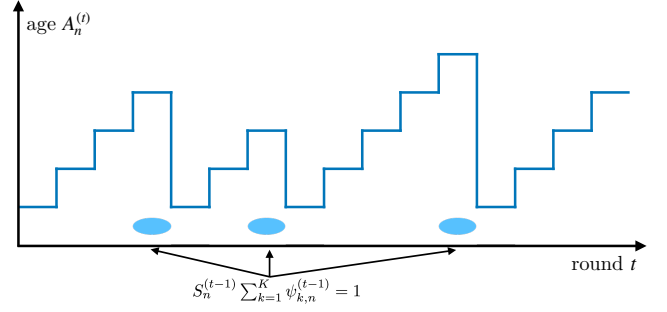


Fig. 1: An illustration of device's information age.

and the set of device selection indicators \mathbf{S} can be mutually inferred.

In order to improve the performance of FL, the status of devices is determined by data quality. It is revealed in [18], [19] that staleness of gradient update may negatively impact learning outcomes. Therefore, the server tends to select the devices with larger age of gradient update for aggregation. In particular, if a device has been skipped for several rounds, its gradient update is relatively informative, and the probability of the server selecting the device should increase. Conversely, if a device was selected in the previous round, the probability for its reselection should decrease. In order to evaluate the staleness, the concept of AoI is introduced [20], [21]. The information age of any device n in round t , denoted by $A_n^{(t)}$, is a integer variable, defined as follows:

$$A_n^{(t)} = \begin{cases} A_n^{(t-1)} + 1, & \text{if } S_n^{(t-1)} \sum_{k=1}^K \psi_{k,n}^{(t-1)} = 0, \\ 1, & \text{if } S_n^{(t-1)} \sum_{k=1}^K \psi_{k,n}^{(t-1)} = 1, \end{cases} \quad (6)$$

where $\psi_{k,n}^{(t)} \in \{0, 1\}$ is the sub-channel assignment indicator. Particularly, $\psi_{k,n}^{(t)} = 1$ indicates device n is assigned to sub-channel k in round t ; $\psi_{k,n}^{(t)} = 0$ otherwise. The above definition shows that the information age of any device in any round is determined by device selection and sub-channel assignment in the previous round. As shown in Fig. 1, if device n was not selected in round $t-1$, i.e., $S_n^{(t-1)} = 0$, or it is not assigned to any sub-channel, i.e., $\sum_{k=1}^K \psi_{k,n}^{(t-1)} = 0$, its information age increments 1; otherwise, its information age is reset to 1.

With this consideration, a large information age implies more informative update, and therefore the device selection should partially depend on the information age. In any round t , $\alpha_n^{(t)}$ defined below is used as a weight to prioritize selecting devices with larger AoI for aggregation:

$$\alpha_n^{(t)} = \frac{A_n^{(t)}}{\sum_{n'=1}^N A_{n'}^{(t)}}. \quad (7)$$

D. Sub-Channel Assignment

According to [6], [12], [22], the convergence rate of FL also depends on the latency of each round. By including computation and communication phases, the time consumption

of any device n assigned to sub-channel k can be expressed as follows¹:

$$T_{k,n}(\tau_{k,n}, P_{k,n}) = T_{k,n}^{\text{cp}}(\tau_{k,n}) + T_{k,n}^{\text{cm}}(P_{k,n}). \quad (8)$$

For device n selected in round t , i.e., $S_n^{(t)} = 1$, a sub-channel is available for transmitting its local model. For the entire FL network, the latency of the t -th aggregation round is decided by the maximum time consumption, as shown in follows:

$$T^{(t)} = \max_{n \in \mathcal{N}_t} \left\{ \sum_{k \in \mathcal{K}} \psi_{k,n}^{(t)} T_{k,n}(\tau_{k,n}, P_{k,n}) \right\}. \quad (9)$$

If any device is assigned to a sub-channel with the enhanced channel gain, the time consumption of this device decreases, and hence, the latency of this round may be reduced. Moreover, the energy consumption of any device n assigned to sub-channel k is given by

$$E_{k,n}(\tau_{k,n}, P_{k,n}) = E_{k,n}^{\text{cp}}(\tau_{k,n}) + E_{k,n}^{\text{cm}}(P_{k,n}). \quad (10)$$

III. PROBLEM FORMULATION

In order to improve the performance of FL in the considered scenario, this paper chooses the convergence time as the target, which is jointly determined by the number of rounds and the time consumption of each round [6]. Therefore, global loss minimization and latency minimization should be jointly considered. This situation can be described as a Stackelberg game, where global loss minimization and latency minimization are considered as leader-level and follower-level problems, respectively.

1) *Leader-Level Problem (Computation)*: In the considered FL algorithm, the local loss at any device n is given by

$$F_n(\mathbf{g}) = \frac{1}{\beta_n} \sum_{i=1}^{\beta_n} \ell(\mathbf{g}; \mathbf{x}_{n,i}, y_{n,i}), \quad (11)$$

where $\ell(\mathbf{w}; \mathbf{x}_{n,i}, y_{n,i})$ is a loss function, $\mathbf{x}_{n,i}$ is the i -th input data of device n , and $y_{n,i}$ is the corresponding label. By including device selection and sub-channel assignment, the aggregated global model in round t is given by

$$\mathbf{g}^{(t)} = \frac{\sum_{n=1}^N S_n^{(t-1)} \sum_{k=1}^K \psi_{k,n}^{(t-1)} \beta_n \mathbf{w}_n^{(t-1)}}{\sum_{n=1}^N S_n^{(t-1)} \sum_{k=1}^K \psi_{k,n}^{(t-1)} \beta_n}. \quad (12)$$

At the computation phase, in order to minimize the global loss, an AoI based device selection problem can be formulated as follows:

$$\min_{\mathbf{S}} \frac{\sum_{n=1}^N \alpha_n^{(t)} S_n^{(t)} \sum_{k=1}^K \psi_{k,n}^{(t)} \sum_{i=1}^{\beta_n} \ell(\mathbf{g}^{(t)}; \mathbf{x}_{n,i}, y_{n,i})}{\sum_{n=1}^N \alpha_n^{(t)} S_n^{(t)} \sum_{k=1}^K \psi_{k,n}^{(t)} \beta_n}, \quad (13)$$

$$\text{s.t. } S_n^{(t)} \in \{0, 1\}, \forall n \in \mathcal{N}, \quad (13a)$$

$$\sum_{n=1}^N S_n^{(t)} \leq K, \quad (13b)$$

Constraints (13a) and (13b) indicate that all devices are available for selection, and the number of selected devices in each round is not greater than the number of available sub-channels.

2) *Follower-Level Problem (Communication)*: Based on the given \mathbf{S} , the set of selected devices \mathcal{N}_t can be obtained. Hence, sub-channel assignment, computational resource allocation, and power allocation are implemented in order to minimize the latency. In any round t , the latency minimization problem can be presented as follows:

$$\min_{\psi, \tau, \mathbf{P}} \max_{n \in \mathcal{N}_t} \left\{ \sum_{k \in \mathcal{K}} \psi_{k,n}^{(t)} T_{k,n}(\tau_{k,n}, P_{k,n}) \right\}, \quad (14)$$

$$\text{s.t. } E_{k,n}(\tau_{k,n}, P_{k,n}) \leq E_n^{\text{max}}, \quad (14a)$$

$$T_{k,n}(\tau_{k,n}, P_{k,n}) \leq T^{\text{max}}, \quad (14b)$$

$$\tau_{k,n} \in [0, 1], P_{k,n} \in [0, P_n^{\text{max}}], \quad (14c)$$

$$\sum_{n \in \mathcal{N}_t} \psi_{k,n}^{(t)} \in \{0, 1\}, \psi_{k,n}^{(t)} \in \{0, 1\}, \quad (14d)$$

$$\sum_{k \in \mathcal{K}} \psi_{k,n}^{(t)} \in \{0, 1\}, \psi_{k,n}^{(t)} \in \{0, 1\}, \quad (14e)$$

where ψ , \mathbf{P} , and τ are the collections of sub-channel assignment indicators, transmit power, and computational resource allocation coefficients, respectively. In constraints (14a) and (14b), the energy limitation E_n^{max} and the maximum tolerance time T^{max} are included, respectively. In constraint (14c), the value ranges of computational resource allocation coefficients and transmit power are presented, respectively. Constraints (14d) and (14e) respectively indicate that each sub-channel can be occupied by maximum one device, and each device can be assigned to maximum one sub-channel. Note that any device or sub-channel is not assigned only if constraints (14a) and (14b) cannot be satisfied by the corresponding assignment.

3) *Stackelberg Equilibrium*: In a Stackelberg game, the leader can predict the strategy of the follower, and then propose its strategy first. For the follower, it can observe the strategy of the leader and provide its response. Specifically, in the formulated Stackelberg game based problem, the leader selects devices for minimizing global loss, and then the follower assigns sub-channels to the selected devices and adjusts computational resource allocation coefficients and transmit power for minimizing latency. By predicting the best response of the follower, the leader can obtain the feasibility of the selected devices in the considered system, and provide the corresponding optimal device selection strategy. This solution follows Stackelberg equilibrium [25], [26], as shown below.

Definition 1. In the formulated Stackelberg game based problem, by respectively defining G_{leader} and G_{follower} as the objective functions of leader-level and follower-level problems, solution $(\mathbf{S}^*, \psi^*, \tau^*, \mathbf{P}^*)$ is the Stackelberg equilibrium if the following conditions hold:

$$\begin{aligned} G_{\text{leader}}(\mathbf{S}^*, \psi^*, \tau^*, \mathbf{P}^*) &\leq G_{\text{leader}}(\mathbf{S}, \psi^*, \tau^*, \mathbf{P}^*), \\ G_{\text{follower}}(\mathbf{S}^*, \psi^*, \tau^*, \mathbf{P}^*) &\leq G_{\text{follower}}(\mathbf{S}^*, \psi, \tau, \mathbf{P}). \end{aligned} \quad (15)$$

In order to achieve Stackelberg equilibrium, the best response of the follower should be obtained, and then the leader can propose its strategy with all possible responses. That is, for any solution of the leader-level problem, i.e., \mathbf{S} , the optimal solution of the follower-level problem, i.e., ψ^* , τ^* , and \mathbf{P}^* , is obtained. Afterwards, the optimal solution of the leader-level problem, i.e., \mathbf{S}^* , is obtained with ψ^* , τ^* , and \mathbf{P}^* .

¹Note that the time consumption for global model transmission from the server to devices is ignored as in [23], [24].

IV. SOLUTION OF FOLLOWER-LEVEL PROBLEM

The formulated follower-level problem in (14) is a non-convex problem with binary constraints. In this section, the follower-level problem is decoupled into two sub-problems and solved iteratively. With fixed sub-channel assignment, the sub-problem related to computational resource allocation and power allocation can be presented as follows:

$$\Gamma = \min_{\tau, P} \{T_{k,n}(\tau_{k,n}, P_{k,n}) | \forall n \in \mathcal{N}_t, \forall k \in \mathcal{K}\}, \quad (16)$$

s.t. (14a), (14c),

where Γ is a $K \times |\mathcal{N}_t|$ matrix containing the minimum time consumptions for all possible device and sub-channel combinations. With the given matrix Γ , the sub-problem related to sub-channel assignment can be presented as follows:

$$\min_{\psi} \max_{n \in \mathcal{N}_t} \left\{ \sum_{k \in \mathcal{K}} \psi_{k,n}^{(t)} \Gamma_{k,n} \right\}, \quad (17)$$

s.t. (14b), (14d), (14e),

where $\Gamma_{k,n}$ is one element of matrix Γ . Note that the time consumption constraint (14b) is included in problem (17), and hence, all combinations of device and sub-channels are feasible for problem (16). Moreover, since matrix Γ is the minimum time consumptions of all possible combinations, if constraint (14b) is still not satisfied in problem (17), the corresponding combination cannot be adopted in sub-channel assignment.

A. Joint Optimization of Power Allocation and Computational Resource Allocation

In this subsection, power allocation and computational resource allocation are jointly optimized with the fixed device selection and sub-channel assignment. It is indicated in problem (16) that the time consumption of any device n assigned to sub-channel k only depends on its own computational resource allocation coefficient $\tau_{k,n}$ and transmit power $P_{k,n}$. Therefore, in order to generate matrix Γ , problem (16) can be divided into multiple sub-problems, where each sub-problem corresponds to one device and sub-channel combination. For any device n assigned to sub-channel k , the sub-problem is given by

$$\min_{\tau_{k,n}, P_{k,n}} \frac{\mu\beta_n}{\tau_{k,n}C_n} + \frac{D(\mathbf{w}_n)}{B \log_2(1 + P_{k,n}|h_{k,n}|^2)} \quad (18)$$

$$\text{s.t. } \kappa_0 \mu \beta_n (\tau_{k,n} C_n)^2 + \frac{P_{k,n} D(\mathbf{w}_n)}{B \log_2(1 + P_{k,n}|h_{k,n}|^2)} \leq E_n^{\max}, \quad (18a)$$

$$\tau_{k,n} \in [0, 1], P_{k,n} \in [0, P_n^{\max}]. \quad (18b)$$

Due to the fact that problem (18) is still non-convex, the traditional optimization methods, such as convex optimization, cannot be directly employed. Therefore, monotonic optimization is introduced to solve this problem. In order to utilize monotonic optimization, the monotonicity of problem (18) should be analyzed. According to [27], the following proposition can be obtained.

Proposition 1. *For any device n assigned to sub-channel k , with computational resource allocation coefficient $\tau_{k,n}$ and*

transmit power $P_{k,n}$, the time consumption $T_{k,n}(\tau_{k,n}, P_{k,n})$ is a decreasing function, while the energy consumption $E_{k,n}(\tau_{k,n}, P_{k,n})$ is an increasing function.

Proof: Refer to Appendix A. ■

According to Proposition 1, it can be proved that the objective function and all constraints in problem (18) are monotonic. Next, this problem should be transformed to a canonical formulation for solving. By defining the power allocation coefficient $p_{k,n} \in [0, 1]$, the objective function in problem (18) is equivalent to maximizing the following function:

$$f(\mathbf{z}_{k,n}) = -\frac{\mu\beta_n}{\tau_{k,n}C_n} - \frac{D(\mathbf{w}_n)}{B \log_2(1 + p_{k,n}P_n^{\max}|h_{k,n}|^2)}, \quad (19)$$

where $\mathbf{z}_{k,n} \in \mathbb{R}_+^{2 \times 1}$ is the collection of the power allocation coefficient and computational resource allocation coefficient, i.e., $\mathbf{z}_{k,n} = \{\tau_{k,n}, p_{k,n}\}$. Similarly, constraint (18a) can be expressed as $g(\mathbf{z}_{k,n}) \leq 0$, where

$$g(\mathbf{z}_{k,n}) = \kappa_0 \mu \beta_n (\tau_{k,n} C_n)^2 + \frac{p_{k,n} P_n^{\max} D(\mathbf{w}_n)}{B \log_2(1 + p_{k,n} P_n^{\max} |h_{k,n}|^2)} - E_n^{\max}. \quad (20)$$

At this stage, problem (18) can be rewritten as follows:

$$\max_{\mathbf{z}_{k,n}} f(\mathbf{z}_{k,n}) \quad (21)$$

$$\text{s.t. } g(\mathbf{z}_{k,n}) \leq 0, \quad (21a)$$

$$\tau_{k,n} \in [0, 1], p_{k,n} \in [0, 1]. \quad (21b)$$

Based on the value range of the computational resource allocation coefficient and power allocation coefficient, a normal set \mathcal{G} can be defined as follows:

$$\mathcal{G} = \{\mathbf{z}_{k,n} \in [0, 1] | g(\mathbf{z}_{k,n}) \leq 0\}. \quad (22)$$

As a result, problem (18) can be presented in a canonical formulation of monotonic optimization, as shown in follows:

$$\max_{\mathbf{z}_{k,n}} f(\mathbf{z}_{k,n}) \quad (23)$$

$$\text{s.t. } \mathbf{z}_{k,n} \in \mathcal{G}. \quad (23a)$$

In problem (23), the objective function $f(\mathbf{z}_{k,n})$ is monotonically increasing with $\mathbf{z}_{k,n}$, and then the optimal solution is located on the boundary of the feasible set \mathcal{G} . However, due to the non-convexity of functions $f(\mathbf{z}_{k,n})$ and $g(\mathbf{z}_{k,n})$, the expression of the boundary cannot be directly derived. In this case, the polyblock outer approximation algorithm in [28] is adopted, which can approach the feasible set \mathcal{G} by constructing polyblock \mathcal{P} . The polyblock outer approximation algorithm is presented in **Algorithm 1**.

As shown in Fig. 2(a), by setting the first vertex $\mathbf{v}^{(1)} \in \mathcal{V}^{(1)}$, the initial polyblock $\mathcal{P}^{(1)}$ can be constructed as the box $[0, 1]$, which contains the feasible set². The projection of $\mathbf{v}^{(1)}$ on the upper boundary of feasible set \mathcal{G} is calculated, denoted by $\phi(\mathbf{v}^{(1)})$. Based on point $\phi(\mathbf{v}^{(1)})$, two new vertices $\tilde{\mathbf{v}}_1^{(1)}$ and

²Note that the initial vertex, i.e., $\tau_{k,n} = 1$ and $p_{k,n} = 1$, may be infeasible for problem (23). However, the optimal solution obtained from Algorithm 1 is the projection of the vertex, which is always included in the feasible set \mathcal{G} .

Algorithm 1 Polyblock Outer Approximation Algorithm

- 1: Initialize initial vertex set $\mathcal{V}^{(1)} = \{\mathbf{v}^{(1)}\}$, where $\mathbf{v}^{(1)} = \{\tau_{k,n}, p_{k,n}\}$, $\tau_{k,n} = 1$ and $p_{k,n} = 1$.
 - 2: Initialize initial polyblock $\mathcal{P}^{(1)}$ with vertex set $\mathcal{V}^{(1)}$.
 - 3: Set ϵ and $\theta = 1$.
 - 4: **if** $|f(\phi(\mathbf{v}^{(\theta)})) - f(\phi(\mathbf{v}^{(\theta-1)}))| > \epsilon$ **then**
 - 5: Obtain $\phi(\mathbf{v}^{(\theta)})$ from Eq. (30).
 - 6: Calculate vertices $\tilde{\mathbf{v}}_1^{(\theta)}$ and $\tilde{\mathbf{v}}_2^{(\theta)}$ as follows:

$$\tilde{\mathbf{v}}_i^{(\theta)} = \mathbf{v}^{(\theta)} - (v_i^{(\theta)} - \phi_i(\mathbf{v}^{(\theta)}))\mathbf{e}_i, \forall i \in \{1, 2\}.$$
 - 7: Update vertex set $\mathcal{V}^{(\theta+1)}$ as follows:

$$\mathcal{V}^{(\theta+1)} = \{\mathcal{V}^{(\theta)} \setminus \mathbf{v}^{(\theta)}\} \cup \{\tilde{\mathbf{v}}_1^{(\theta)}, \tilde{\mathbf{v}}_2^{(\theta)}\}.$$
 - 8: Construct polyblock $\mathcal{P}^{(\theta+1)}$ with vertex set $\mathcal{V}^{(\theta+1)}$.
 - 9: Find vertex $\mathbf{v}^{(\theta+1)}$ from $\mathcal{V}^{(\theta+1)}$, where

$$\mathbf{v}^{(\theta+1)} = \operatorname{argmax}\{f(\phi(\mathbf{v})) | \mathbf{v} \in \mathcal{V}^{(\theta+1)}\}.$$
 - 10: Set $\theta = \theta + 1$.
 - 11: **end if**
 - 12: Set $\mathbf{z}_{k,n}^* = \phi(\mathbf{v}^{(\theta)})$.
-

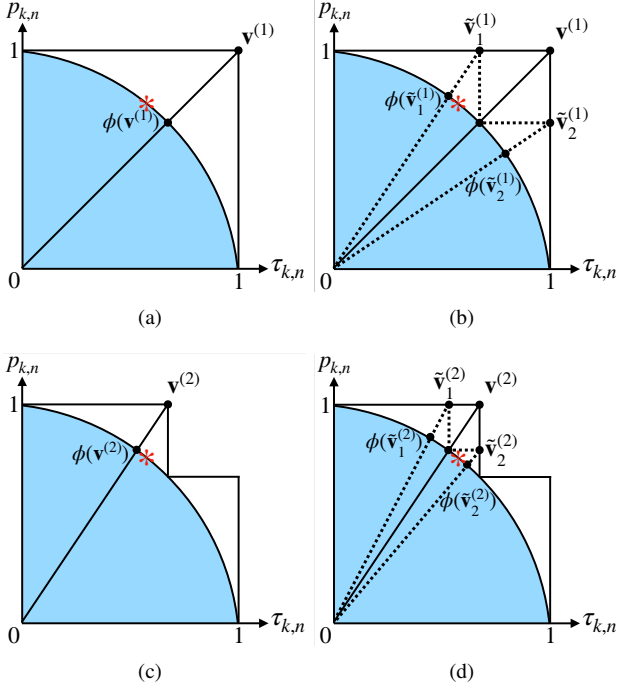


Fig. 2: An illustration of the polyblock outer approximation algorithm. The blue area is the feasible set \mathcal{G} , and the red star is the optimal point.

$\tilde{\mathbf{v}}_2^{(1)}$ can be obtained to replace $\mathbf{v}^{(1)}$, as shown in Fig. 2(b). The new vertices are calculated as follows:

$$\tilde{\mathbf{v}}_i^{(1)} = \mathbf{v}^{(1)} - (v_i^{(1)} - \phi_i(\mathbf{v}^{(1)}))\mathbf{e}_i, \forall i \in \{1, 2\}, \quad (24)$$

where $v_i^{(1)}$ is the i -th element of $\mathbf{v}^{(1)}$, $\phi_i(\mathbf{v}^{(1)})$ is the i -th element of $\phi(\mathbf{v}^{(1)})$, and \mathbf{e}_i is the i -th unit vector. At this stage,

a new polyblock $\mathcal{P}^{(2)}$ is obtained, where $\mathcal{G} \subset \mathcal{P}^{(2)} \subset \mathcal{P}^{(1)}$, as shown in Fig. 2(c). The vertex set of $\mathcal{P}^{(2)}$ is updated as follows:

$$\mathcal{V}^{(2)} = \{\mathcal{V}^{(1)} \setminus \mathbf{v}^{(1)}\} \cup \{\tilde{\mathbf{v}}_1^{(1)}, \tilde{\mathbf{v}}_2^{(1)}\}. \quad (25)$$

After that, the optimal vertex is selected from vertex set $\mathcal{V}^{(2)}$ and denoted by $\mathbf{v}^{(2)}$, which satisfies the following condition:

$$\mathbf{v}^{(2)} = \operatorname{argmax}\{f(\phi(\mathbf{v})) | \mathbf{v} \in \mathcal{V}^{(2)}\}. \quad (26)$$

That is, the projection of the optimal vertex can achieve the maximum value of the objective function, i.e., (19). For example, Fig. 2(c) shows the case that $\tilde{\mathbf{v}}_1^{(1)}$ is selected as the optimal vertex $\mathbf{v}^{(2)}$. This process is repeated, and a smaller polyblock $\mathcal{P}^{(3)} \subset \mathcal{P}^{(2)}$ is constructed based on vertex $\mathbf{v}^{(2)}$, as shown in Fig. 2(d). This algorithm is completed if the following condition is satisfied:

$$|f(\phi(\mathbf{v}^{(\theta)})) - f(\phi(\mathbf{v}^{(\theta-1)}))| \leq \epsilon, \quad (27)$$

where ϵ is the error tolerance. The output $\mathbf{z}_{k,n}^* = \phi(\mathbf{v}^{(\theta)})$ is the optimal solution of problem (23).

The projection of any vertex $\mathbf{v}^{(\theta)}$ satisfies the following condition:

$$\phi(\mathbf{v}^{(\theta)}) = \zeta \mathbf{v}^{(\theta)}, \quad (28)$$

where $\zeta \in (0, 1)$ is a ratio coefficient obtained as follows:

$$\begin{aligned} \zeta &= \max\{\tilde{\zeta} \in (0, 1) | \tilde{\zeta} \mathbf{v}^{(\theta)} \in \mathcal{G}\} \\ &= \max\{\tilde{\zeta} \in (0, 1) | g(\tilde{\zeta} \mathbf{v}^{(\theta)}) \leq 0, \tilde{\zeta} \mathbf{v}^{(\theta)} \in [0, 1]\}. \end{aligned} \quad (29)$$

Since that $g(\tilde{\zeta} \mathbf{v}^{(\theta)})$ is a monotonic increasing function, ζ satisfies $g(\zeta \mathbf{v}^{(\theta)}) = 0$, which can be written as follows:

$$\kappa_0 \mu \beta_n (\zeta v_1^{(\theta)} C_n)^2 + \frac{\zeta v_2^{(\theta)} P_n^{\max} D(\mathbf{w}_n)}{B \log_2(1 + \zeta v_2^{(\theta)} P_n^{\max} |h_{k,n}|^2)} = E_n^{\max}. \quad (30)$$

The closed-form expression of ζ cannot be presented, but this nonlinear equation can be solved by multiple numerical solvers, such as MATLAB. It is worth pointing out that during **Algorithm 1**, with any given vertex $\mathbf{v}^{(\theta)} = \{v_1^{(\theta)}, v_2^{(\theta)}\}$, where $\theta \geq 2$, condition $\zeta \in (0, 1)$ is always satisfied. When $\theta = 1$, $\zeta = 1$ may be obtained with vertex $\mathbf{v}^{(1)} = \{v_1^{(1)}, v_2^{(1)}\}$, which means the feasible set \mathcal{G} includes the first vertex. That is, the energy consumption constraint $g(\mathbf{z}_{k,n}) < 0$ can be satisfied with any $\tau_{k,n}$ and $p_{k,n}$ in $[0, 1]$. In this case, the optimal solution is obtained by $\mathbf{z}_{k,n}^* = \mathbf{v}^{(1)}$.

B. Matching based Sub-Channel Assignment

Based on **Algorithm 1**, the minimum time consumptions of all selected devices in all sub-channels is obtained in matrix Γ . In this subsection, a matching based algorithm is proposed to solve the binary integer programming problem in (17), where matrix Γ is utilized to construct the preference list.

In the sub-channel assignment problem, the set of selected devices, i.e., \mathcal{N}_t , is available. Moreover, as revealed in Section V, in order to maximize the weighted global loss, the number of selected devices should be maximized in each round, i.e., $|\mathcal{N}_t| = K$. In this case, \mathcal{N}_t and \mathcal{K} are two disjoint sets with the same size, and hence, this scenario can be considered as

a one-to-one matching Ψ from \mathcal{N}_t to \mathcal{K} . Based on matrix Γ , in any matching Ψ , the utility of device n assigned to sub-channel k can be presented as follows:

$$U_n(\Psi) = \begin{cases} U_{\max}, & \text{if } \Gamma_{k,n} > T^{\max}, \\ \Gamma_{k,n}, & \text{otherwise,} \end{cases} \quad (31)$$

where U_{\max} is a large constant indicating that the assignment of device n and sub-channel k is infeasible. In the matching phase, all devices and sub-channels are matched, and hence, the utility of any sub-channel is equal to the utility of the occupied device, i.e., $U_k(\Psi) = U_{\Psi(k)}(\Psi), \forall k \in \mathcal{K}$. By calculating the utility, the preference list of any player can be established. Due to the fact that the formulated sub-channel assignment problem is a latency minimization problem, the preference of any device n is defined as follows:

$$(k, \Psi) \prec_n (k', \Psi') \Rightarrow U_n(\Psi) > U_n(\Psi'). \quad (32)$$

The above function indicates that device n is willing to be assigned to sub-channel k' in matching Ψ' , rather than k in matching Ψ , since its utility can be strictly decreased by assigning from k to k' . Similarly, the preference of any sub-channel k can be defined as follows:

$$(n, \Psi) \prec_k (n', \Psi') \Rightarrow U_k(\Psi) > U_k(\Psi'). \quad (33)$$

Since all players are matched, the considered case follows the concept of two-sided exchange matchings [29]. Therefore, when any device intends to be assigned to a sub-channel, it needs to exchange with another device occupying this sub-channel, instead of directly joining this sub-channel. A notation $\Psi_{n'}^n$ is introduced to represent the case where exactly two devices n and n' are swapped in any matching Ψ , which is defined as follows:

$$\Psi_{n'}^n(l) = \begin{cases} \Psi(l), & l \neq n, n' \\ \Psi(n') = k', & l = n \\ \Psi(n) = k, & l = n' \end{cases} \quad (34)$$

where $\Psi_{n'}^n$ only replaces two pairs defined by $\Psi(n) = k$ and $\Psi(n') = k'$ into $\Psi(n) = k'$ and $\Psi(n') = k$, respectively. It is indicated that any swap operation involves four players, and hence, the swap operation should be approved by the involved players. Specifically, at least one player $i \in \{n, n', k, k'\}$ can reduce its utility without increasing the others' utilities. In this case, a swap-blocking pair (n, n') is formed, which is defined as follows [30]:

Definition 2. A swap-blocking pair (n, n') is confirmed if and only if the following conditions hold

- 1) $U_i(\Psi_{n'}^n) \leq U_i(\Psi), \forall i \in \{n, n', k, k'\}$;
- 2) At least one inequality above is strict.

By searching swap-blocking pairs, a matching based sub-channel assignment algorithm can be proposed in **Algorithm 2**. The proposed algorithm can be started from any initial matching. During the algorithm, an active device n is selected and try to sequentially swap with all other devices. If a swap-blocking pair (n, n') is formed, i.e., the conditions in Definition 2 are satisfied, the new matching $\Psi_{n'}^n$ is recorded, and the algorithm continues. The main loop of **Algorithm 2**

Algorithm 2 Sub-Channel Assignment Algorithm

- 1: **Initialization:**
 - 2: Initialize initial matching Ψ by randomly pairing all devices and sub-channels.
 - 3: **Main Loop:**
 - 4: **for** $n \in \mathcal{N}_t$ **do**
 - 5: Device n makes a proposal to exchange with device $n' \in \mathcal{N}_t$, where $n \neq n'$.
 - 6: **if** (n, n') is a swap-blocking pair **then**
 - 7: Matching $\Psi_{n'}^n$ is approved.
 - 8: Devices n and n' exchange sub-channels.
 - 9: Set $\Psi = \Psi_{n'}^n$
 - 10: **end if**
 - 11: **end for**
 - 12: The main loop is repeated until no swap-blocking pair can be found in a complete round.
-

executes repeatedly. When the last device has searched for all other devices, the first device becomes the active device again. The algorithm ends if no swap blocking pair can be found in a full round of the main loop. At this stage, the final matching is outputted as the solution of problem (17). If any device n assigned to sub-channel k cannot satisfy constraint (14b), its sub-channel assignment indicator is set to $\psi_{k,n} = 0$.

In this subsection, the properties of the proposed matching based sub-channel assignment algorithm, including complexity, convergence, and stability, are analyzed.

1) *Complexity:* The computational complexity of the proposed matching based algorithm can be presented by considering the worst case.

Proposition 2. With the given number of main loops C , the computational complexity of the matching based sub-channel assignment algorithm is $\mathcal{O}(CK^2)$.

Proof: The worst case can be defined as the situation that all devices need to search all other devices. In the main loop, K devices can play the role of active devices, and each one searches $K-1$ devices. Hence, $K(K-1)$ times of calculations should be performed in one loop. With the given number of main loops C , the complexity of the proposed algorithm can be expressed as $\mathcal{O}(CK^2)$. ■

2) *Convergence:* The convergence of the proposed sub-channel assignment algorithm is presented as follows.

Proposition 3. From any initial matching, the matching based sub-channel assignment algorithm is guaranteed to converge to a stable matching.

Proof: During the proposed algorithm, the matching is transformed as follows:

$$\Psi^{\text{initial}} \rightarrow \Psi^{(1)} \rightarrow \Psi^{(2)} \rightarrow \dots \rightarrow \Psi^{\text{final}}. \quad (35)$$

Assume that $\Psi^{(a)}$ and $\Psi^{(b)}$ are two adjacent matching, i.e., $\Psi^{(a)} \rightarrow \Psi^{(b)}$, one swap-blocking pair is found among the transformation. According to Definition 2, at least one player can achieve less utility, and the utilities of all players cannot

be increased. The following inequality is always satisfied:

$$\sum_{i \in \mathcal{N}_i} U_i(\Psi^{(a)}) > \sum_{i \in \mathcal{N}_i} U_i(\Psi^{(b)}). \quad (36)$$

Therefore, the matching transformation in (35) cannot be reversed. With the finite number of devices and sub-channels, the number of possible matchings is finite and equal to the Bell number [31]. Therefore, the final matching can be always obtained. ■

3) *Stability*: The stability of the proposed matching based algorithm follows the following definition [29], [30]:

Definition 3. A matching Ψ is two-sided exchange-stable (2ES) if and only if there is no further swap-blocking pair.

Based on the above definition, the stability of the matching based sub-channel assignment algorithm can be expressed as follows:

Proposition 4. Any final matching obtained from Algorithm 2 is 2ES.

Proof: If the final matching obtained from Algorithm 2 is not 2ES, there exists at least one swap-blocking pair, which can further reduce the sum utility of all devices. However, it contradicts the conditions for completing the algorithm. This proposition is proved. ■

V. SOLUTION OF LEADER-LEVEL PROBLEM

In order to solve the formulated global loss minimization problem in (13), the impact of device selection on the expected convergence rate should be analyzed. By employing the gradient descent method, with the given global model $\mathbf{g}^{(t)}$, device n can update the local model as follows:

$$\mathbf{w}_n^{(t)} = \mathbf{g}^{(t)} - \frac{\lambda}{\beta_n} \sum_{i=1}^{\beta_n} \nabla \ell(\mathbf{g}^{(t)}; \mathbf{x}_{n,i}, y_{n,i}), \quad (37)$$

where λ is the learning rate. After that, all selected devices transmit the updated local model $\mathbf{w}_n^{(t)}$ to the server for aggregation. The update of the global model in round t can be written as follows:

$$\begin{aligned} \mathbf{g}^{(t+1)} &= \frac{\sum_{n=1}^N S_n^{(t)} \sum_{k=1}^K \psi_{k,n}^{(t)} \beta_n \mathbf{w}_n^{(t)}}{\sum_{n=1}^N S_n^{(t)} \sum_{k=1}^K \psi_{k,n}^{(t)} \beta_n} \\ &= \mathbf{g}^{(t)} - \frac{\lambda \sum_{n=1}^N S_n^{(t)} \sum_{k=1}^K \psi_{k,n}^{(t)} \sum_{i=1}^{\beta_n} \nabla \ell(\mathbf{g}^{(t)}; \mathbf{x}_{n,i}, y_{n,i})}{\sum_{n=1}^N S_n^{(t)} \sum_{k=1}^K \psi_{k,n}^{(t)} \beta_n} \\ &= \mathbf{g}^{(t)} - \lambda [\nabla F(\mathbf{g}^{(t)}) - \hat{\mathbf{g}}], \end{aligned} \quad (38)$$

where

$$\nabla F(\mathbf{g}^{(t)}) = \frac{\sum_{n=1}^N \sum_{i=1}^{\beta_n} \nabla \ell(\mathbf{g}^{(t)}; \mathbf{x}_{n,i}, y_{n,i})}{\sum_{n=1}^N \beta_n}, \quad (39)$$

and

$$\hat{\mathbf{g}} \triangleq \nabla F(\mathbf{g}^{(t)}) - \frac{\sum_{n=1}^N S_n^{(t)} \sum_{k=1}^K \psi_{k,n}^{(t)} \sum_{i=1}^{\beta_n} \nabla \ell(\mathbf{g}^{(t)}; \mathbf{x}_{n,i}, y_{n,i})}{\sum_{n=1}^N S_n^{(t)} \sum_{k=1}^K \psi_{k,n}^{(t)} \beta_n}. \quad (40)$$

To derive the expected convergence rate of FL in any round t , based on [7], [8], [32], the following assumptions are considered:

1) With respect to \mathbf{g} , the gradient $\nabla F(\mathbf{g})$ of $F(\mathbf{g})$ is uniformly Lipschitz continuous, i.e.,

$$\|\nabla F(\mathbf{g}^{(t+1)}) - \nabla F(\mathbf{g}^{(t)})\| \leq L \|\mathbf{g}^{(t+1)} - \mathbf{g}^{(t)}\|, \quad (41)$$

where L is a positive constant, and $\|\bullet\|$ is the norm operator.

2) The following inequality is satisfied with any device n and sample i :

$$\|\nabla \ell(\mathbf{g}^{(t)}; \mathbf{x}_{n,i}, y_{n,i})\|^2 \leq \rho \|\nabla F(\mathbf{g}^{(t)})\|^2, \quad (42)$$

where ρ is a non-negative constant.

It is worth pointing out that the above assumptions are commonly considered in the FL related optimization, and can be satisfied by widely adopted loss functions. Based on these assumptions, the following proposition can be derived.

Proposition 5. In the case that device selection and sub-channel assignment satisfy $S_n^{(t)} = \sum_{k=1}^K \psi_{k,n}^{(t)}$, $\forall n \in \mathcal{N}$, with the learning rate $\lambda = 1/L$ and the optimal global model \mathbf{g}^* , the upper bound of $\mathbb{E}[F(\mathbf{g}^{(t+1)}) - F(\mathbf{g}^*)]$ in round t can be presented as follows:

$$\begin{aligned} \mathbb{E}[F(\mathbf{g}^{(t+1)}) - F(\mathbf{g}^*)] &\leq \mathbb{E}[F(\mathbf{g}^{(t)}) - F(\mathbf{g}^*)] - \frac{1}{2L} \|\nabla F(\mathbf{g}^{(t)})\|^2 \\ &\quad + \frac{2\rho \|\nabla F(\mathbf{g}^{(t)})\|^2}{L \sum_{n=1}^N \beta_n} \sum_{n=1}^N \beta_n \left(1 - S_n^{(t)} \sum_{k=1}^K \psi_{k,n}^{(t)}\right). \end{aligned} \quad (43)$$

Proof: Refer to Appendix B. ■

It is indicated that the convergence rate in any round t is bounded by three terms. The first term, i.e., $\mathbb{E}[F(\mathbf{g}^{(t)}) - F(\mathbf{g}^*)]$, is the expected upper bound in the previous round. The second term is the norm of the global model gradient from the previous round. The third term is related to device selection, where the status of devices in round t , i.e., $S_n^{(t)}$, is included. Proposition 5 indicates the expected gap between the global loss in round t and the optimal loss. In this case, the train loss minimization problem in (13) can be achieved by minimizing the expected gap. Moreover, since that the first two terms do not include device selection, they can be treated as constants. Meanwhile, the term $\frac{2\rho \|\nabla F(\mathbf{g}^{(t)})\|^2}{L \sum_{n=1}^N \alpha_n^{(t)} \beta_n}$ is positive and not effected by device selection, and hence, it can be removed. By including the AoI based weight $\alpha_n^{(t)}$, the objective function of the leader-level problem (13) can be reformulated as follows:

$$\min_{\mathbf{S}} \sum_{n=1}^N \beta_n \left(1 - \alpha_n^{(t)} S_n^{(t)} \sum_{k=1}^K \psi_{k,n}^{(t)}\right) \quad (44)$$

By removing the constant term $\sum_{n=1}^N \beta_n$, the leader-level problem (13) can be equivalently transformed as follows:

$$\begin{aligned} \max_{\mathbf{S}} \quad & \sum_{n=1}^N \alpha_n^{(t)} \beta_n S_n^{(t)} \sum_{k=1}^K \psi_{k,n}^{(t)} \\ \text{s.t.} \quad & (13a), (13b). \end{aligned} \quad (45)$$

Algorithm 3 Device Selection Algorithm

- 1: **Initialization:**
 - 2: Generate list $\mathcal{Q}^{(t)}$ based on (46).
 - 3: Initialize set \mathcal{N}_t by selecting the first K devices from $\mathcal{Q}^{(t)}$.
 - 4: **Main Loop:**
 - 5: Obtain sub-channel assignment from **Algorithm 2**.
 - 6: **if** $\sum_{n \in \mathcal{N}_t} \sum_{k=1}^K \psi_{k,n}^{(t)} < K$ **and** $(N) \notin \mathcal{N}_t$ **then**
 - 7: **for** $n \in \mathcal{N}_t$ **do**
 - 8: **if** $\sum_{k=1}^K \psi_{k,n}^{(t)} = 0$ **then**
 - 9: Remove device n from set \mathcal{N}_t .
 - 10: Add the next unselected device from list $\mathcal{Q}^{(t)}$.
 - 11: **end if**
 - 12: **end for**
 - 13: **end if**
 - 14: The main loop is repeated until \mathcal{N}_t does not change in two consecutive loops.
-

The above problem can be treated as a weighted device selection problem, where both AoI and data size play the role of weight factors. For example, the weight of device n can be expressed by $\alpha_n^{(t)} \beta_n$. Therefore, the server can order and select devices based on the priority. In any round t , all devices can be sorted and recorded in a list $\mathcal{Q}^{(t)}$, which satisfies the following condition:

$$\alpha_{(1)}^{(t)} \beta_{(1)} \geq \alpha_{(2)}^{(t)} \beta_{(2)} \geq \dots \geq \alpha_{(N)}^{(t)} \beta_{(N)}, \quad (46)$$

where (1) and (N) denote the devices with the highest and lowest priority, respectively. On the other hand, for maximizing the utility, the server tends to select more devices, and hence, constraint (13b) can be rewritten as $\sum_{n=1}^N S_n^{(t)} = K$. That is, the number of selected devices is equal to the number of available sub-channels. According to the list $\mathcal{Q}^{(t)}$, problem (45) can be solved by **Algorithm 3**. In the proposed device selection algorithm, K devices with the highest priority are selected in the initialization phase. During **Algorithm 3**, any device not assigned to a sub-channel will be replaced, until all selected devices have been assigned to sub-channels, or all devices in list $\mathcal{Q}^{(t)}$ have been adopted.

VI. SIMULATION RESULTS

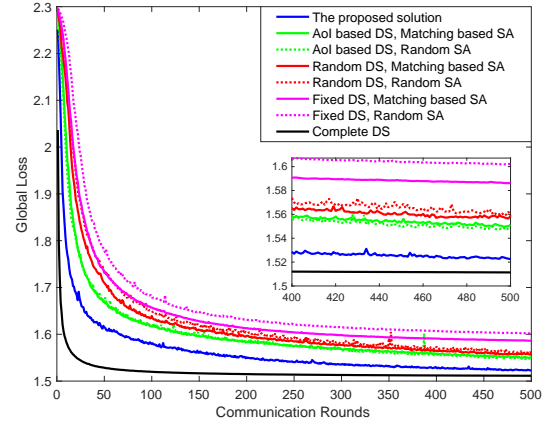
In this section, the performance of the proposed solution is simulated and demonstrated. Multiple device selection (DS) schemes are considered as benchmarks, as shown in follows:

- With AoI based DS, the server selects devices based on the list in (46).
- With random DS, the server selects devices randomly.
- With fixed DS, the same devices are selected in all rounds.

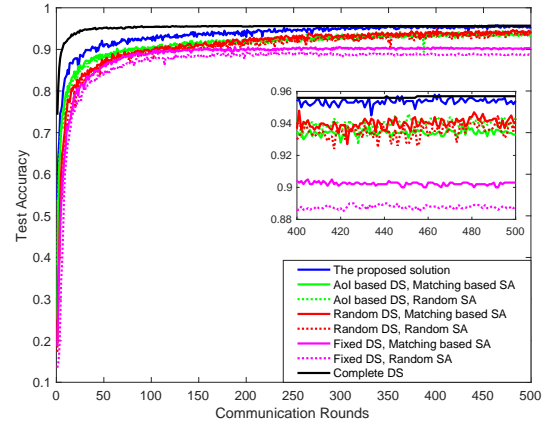
Note that in above schemes, the proposed resource allocation algorithm in Algorithm 1 is adopted. The selected devices can participate in the aggregation of this round only if the time and energy limitations are satisfied. Moreover, the random sub-channel assignment (SA) scheme directly exploits the initial matching in Algorithm 2. The parameters of the simulation are shown in Table I.

TABLE I: Table of Parameters

Radius of the disc	500 m
Carrier frequency	$f = 1$ GHz
AWGN spectral density	$N_0 = -174$ dBm/Hz
Path loss exponent	$\alpha = 3.76$
Bandwidth for each sub-channel	$B = 1$ MHz
Maximum transmit power	10 dBm
Power consumption coefficient	$\kappa_0 = 10^{-28}$
CPU cycles for each bit of tasks	$\mu = 10^7$
Computation capacity	$C_n = 1$ GHz
Size of local model	$D(w) = 1$ Mbit
Maximum energy consumption	$E_n^{\max} = 0.05$ Joule
Maximum time consumption	$T^{\max} = 10$ s
Error tolerance	$\epsilon = 0.01$
Learning rate	$\lambda = 0.01$



(a)



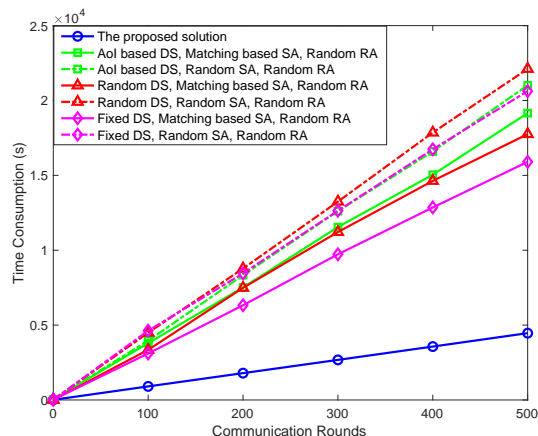
(b)

 Fig. 3: The performance of FL on IID data. $N = 64$, and $K = 8$.

Fig. 3 presents the global loss and the corresponding test accuracy of different schemes, where the probability of device selection is shown in Table II. The complete DS scheme is included to show the upper bound, where all devices are selected for the aggregation. It can be found that with the limited number of sub-channels, the proposed solution can achieve the best performance, including the lowest global loss, the fastest convergence rate, and the highest test accuracy. Suppose that the target test accuracy is 94%, the required number of communication rounds for the proposed solution

TABLE II: Distribution of the probability to select different number of devices in Fig. 3

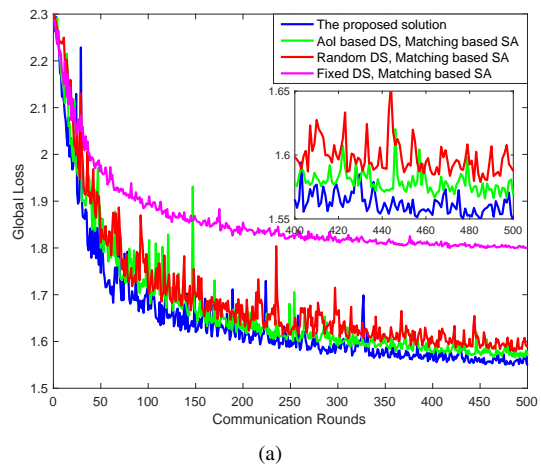
Number of selected devices	0	1	2	3	4	5	6	7	8
The proposed solution	0	0	0	0	0	0	0	0	100%
AoI based DS and matching based SA	0	0	0	1%	11.2%	35.8%	38%	12.8%	1.2%
AoI based DS and random SA	0.6%	3.6%	15.8%	25%	30.6%	19.6%	3.8%	1%	0
Random DS and matching based SA	0	0	0	0	1%	20.6%	43.6%	31.8%	3%
Random DS and random SA	0	1.4%	9.6%	20.2%	30.6%	25.4%	11.4%	1.4%	0
Fixed DS and matching based SA	0	0	0	0	0.4%	9%	50%	37.2%	3.4%
Fixed DS and random SA	0	0	0.2%	3.8%	27.6%	31.8%	27.8%	8%	8%

Fig. 4: The impact of device selection, sub-channel assignment, and resource allocation on latency. $N = 64$, and $K = 8$.

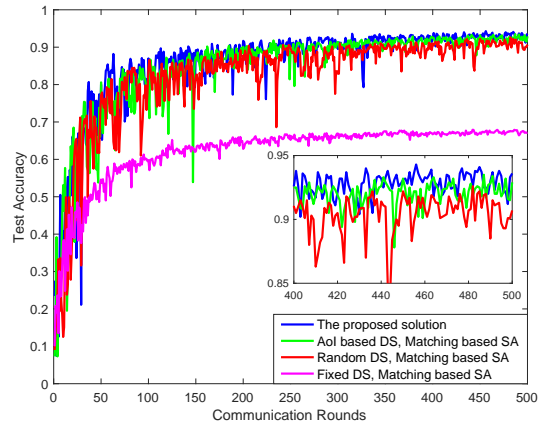
and random DS with matching based SA is 142 and 337, respectively. The AoI based DS is able to outperform random DS, especially in convergence rate. In the fixed DS, the size of dataset is obviously smaller than other schemes, which leads to the worst performance. By comparing matching based SA and random SA, it can be found the proposed matching based algorithm can improve the performance of FL. This is because the matching based SA can significantly increase the number of selected devices in each communication round, as shown in Table II. It is worth to highlight the proposed device selection algorithm can replace devices, and hence, the number of selected devices is always equal to the number of sub-channels.

In Fig. 4, random resource allocation (RA) is employed to show the performance of the proposed solution, where the time consumption limitation in constraint (14b) is ignored. It is indicated that the proposed RA algorithm and SA algorithm can significantly reduce the time consumption. Based on the proposed solution, the average latency of each communication is 8.9246 s, while the average latency of other schemes is around 36 s. On the other hand, the proposed matching based SA algorithm can decrease the latency for all DS schemes. The reduction of time consumption with AoI based DS is relatively less than other schemes, since AoI based DS tends to select the devices with large AoI that usually have poor channel conditions.

The improvement of the proposed solution on non-IID data is demonstrated in Fig. 5, where the 1-class non-IID case in [33] is employed. It can be found that compared to other schemes, the proposed solution can still achieve the best performance, and the test accuracy is 3% higher than that of



(a)



(b)

Fig. 5: The performance of FL on non-IID data. $N = 64$, and $K = 8$.

random DS. Moreover, AoI based DS can achieve higher test accuracy than random DS within 500 communication rounds, which is different from IID data. The performance of fixed DS is obviously worse than that on IID data. This is because only 8 devices can be selected, and then at least 2 digits are missed during training with the MNIST database.

Fig. 6 presents the effect of available sub-channels in the considered FL scenario. With the raising number of available sub-channels, the global loss of all schemes is decreasing, and the corresponding test accuracy is increasing. Compared to other schemes, the proposed solution can achieve the best performance for all sub-channel numbers. It is worth to highlight that the performance of AoI based DS is worse than random DS when the sub-channel number is 2, since the AoI

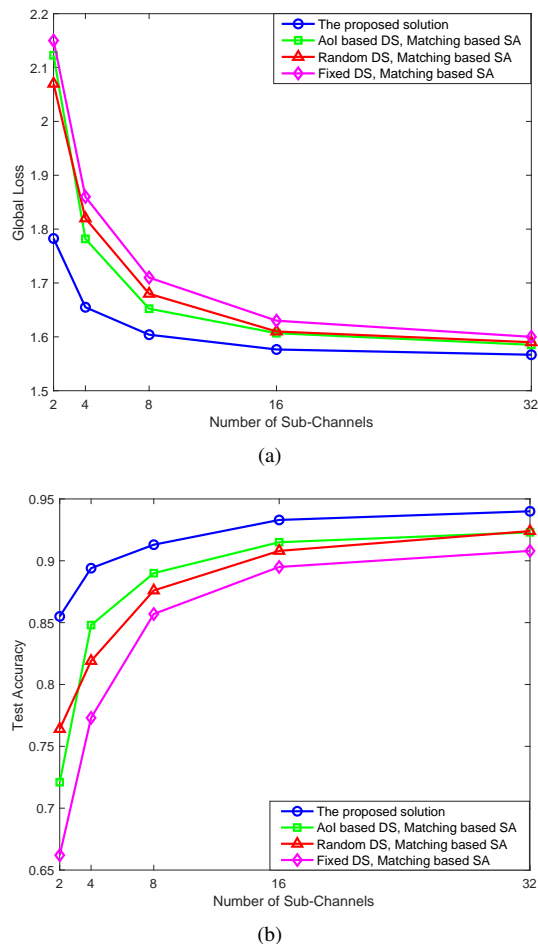


Fig. 6: The performance of FL with different number of sub-channels. $N = 64$, and communication rounds are 200.

based DS scheme always tries to select devices with poor channel conditions repeatedly. When the number of available sub-channels is greater than or equal to 4, AoI based DS can outperform random DS. The gap between AoI based DS and random DS is reduced with the increasing sub-channel number.

Fig. 7 is an example showing the changes of information age in the proposed solution and the random DS scheme. It can be found that by utilizing the proposed solution, the information age of all devices is relatively small, which means devices are equally selected. In particular, the largest information age is 10 in the proposed solution. However, in the random DS scheme, the information age of most devices can be 20, and for the device with poor channel gain, such as device 5, the information age can be 50. Furthermore, the test accuracy shows that the proposed scheme can achieve nearly 1% improvement.

VII. CONCLUSIONS

This paper investigated FL in a practical wireless communication scenario with limited sub-channels and resources. For minimizing the global loss, the AoI based device selection scheme was proposed to select devices in each communication round, and computational resource allocation, power allocation, and sub-channel assignment were jointly considered to

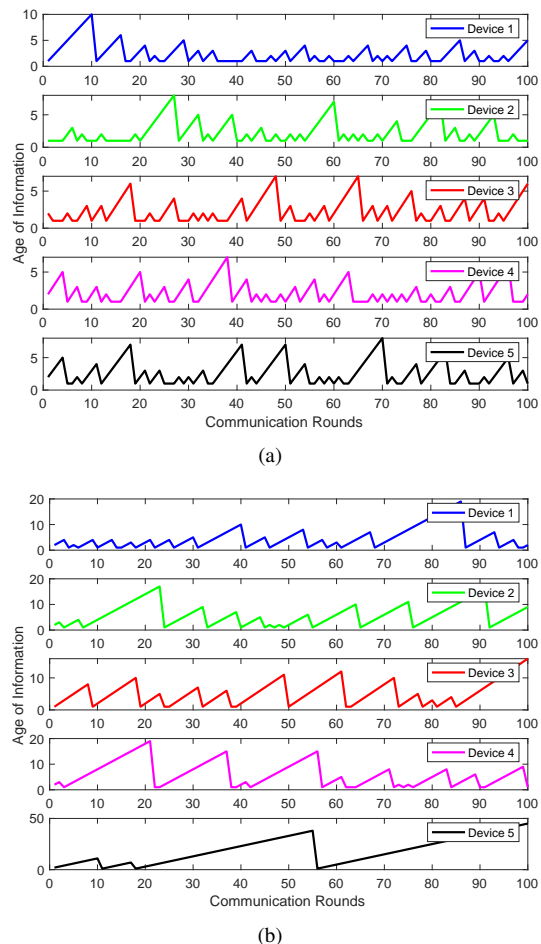


Fig. 7: The performance of FL with non-IID data and unequally size. $N = 5$, and $K = 2$. (a) The proposed solution, 96.5% test accuracy. (b) Random DS, 95.6% test accuracy.

minimize the latency of each round. The monotonicity of the resource allocation problem was analyzed, and then a monotonic optimization based algorithm was developed to find the optimal solution. With the given solution of resource allocation, a matching based algorithm was proposed to solve the sub-channel assignment problem. For the global loss function minimization problem, the upper bound of convergence rate was derived, and AoI was included as part of the weight. By ordering devices according to their priorities, a device selection algorithm was proposed. Simulation results demonstrated that the proposed scheme is able to achieve the near optimal solution, and can significantly improve the test accuracy and latency.

ACKNOWLEDGEMENT

We would like to acknowledge the support of the University of Surrey 5GIC & 6GIC (<https://www.surrey.ac.uk/institute-communication-systems/5g-6g-innovation-centre>) members for this work.

APPENDIX A: PROOF OF PROPOSITION 1

It is obvious that the time consumption of any device n in sub-channel k , i.e., $T_{k,n}(\tau_{k,n}, P_{k,n})$, is monotonically

decreasing with variables $\tau_{k,n}$ and $P_{k,n}$. In terms of the energy consumption, as shown in constraint (18a), the monotonicity can be proved by two parts. The first term, i.e., $\kappa_0\mu\beta_n(\tau_{k,n}C_n)^2$, is the energy consumption for computation, which is monotonically increasing with the computational resource allocation coefficient. The second term is the energy consumption for communication, which can be presented as follows:

$$E_{k,n}^{\text{cm}}(P_{k,n}) = \frac{P_{k,n}D(\mathbf{w}_n)}{B \log_2(1 + P_{k,n}|h_{k,n}|^2)}. \quad (47)$$

The derivative of the above function is

$$\frac{\partial E_{k,n}^{\text{cm}}(P_{k,n})}{\partial P_{k,n}} = \frac{\ln(2)D(\mathbf{w}_n)}{B(1 + P_{k,n}|h_{k,n}|^2) \ln^2(1 + P_{k,n}|h_{k,n}|^2)} \times [(1 + P_{k,n}|h_{k,n}|^2) \ln(1 + P_{k,n}|h_{k,n}|^2) - P_{k,n}|h_{k,n}|^2]. \quad (48)$$

Since the first term of the above function is always greater than zero, the monotonicity of function $E_{k,n}^{\text{cm}}(P_{k,n})$ depends on the term in the square bracket. Particularly, $E_{k,n}^{\text{cm}}(P_{k,n})$ is an increasing function if the following inequality can be proved:

$$(1 + P_{k,n}|h_{k,n}|^2) \ln(1 + P_{k,n}|h_{k,n}|^2) - P_{k,n}|h_{k,n}|^2 \geq 0. \quad (49)$$

Suppose $\theta_{k,n} \triangleq \frac{1}{P_{k,n}|h_{k,n}|^2 + 1}$, the above inequality is equivalent to the following inequality:

$$\frac{1}{\theta_{k,n}}(\theta_{k,n} - 1 - \ln \theta_{k,n}) \geq 0. \quad (50)$$

Due to the fact that $\theta_{k,n} > 0$ is satisfied, $\ln \theta_{k,n} \leq \theta_{k,n} - 1$ can be obtained, and hence, the above inequality always holds, which indicates that $E_{k,n}^{\text{cm}}(P_{k,n})$ is an increasing function. Since that energy consumptions for computation and communication are two increasing functions, the total energy consumption $E_{k,n}(\tau_{k,n}, P_{k,n})$ is also an increasing function. This proposition is proved.

APPENDIX B: PROOF OF PROPOSITION 5

In order to prove this proposition, an auxiliary function is defined as follows:

$$G(\mathbf{g}) = \frac{L}{2} \mathbf{g}^\top \mathbf{g} - F(\mathbf{g}). \quad (51)$$

With respect to \mathbf{g} , the second-order partial derivative of the above function is given by

$$\frac{\partial^2 G(\mathbf{g})}{\partial \mathbf{g}^2} = L - \frac{\partial^2 F(\mathbf{g})}{\mathbf{g}^2}. \quad (52)$$

Since $F(\mathbf{g})$ satisfies the uniformly Lipschitz condition, the above function is always greater than or equal to zero, and hence, $G(\mathbf{g})$ is a convex function. By utilizing the second-order Taylor series expansion, the following inequality can be obtained:

$$G(\mathbf{g}^{(t+1)}) \geq G(\mathbf{g}^{(t)}) + (\mathbf{g}^{(t+1)} - \mathbf{g}^{(t)})^\top \nabla G(\mathbf{g}^{(t)}). \quad (53)$$

From (51), the above inequality can be equivalently transformed as follows:

$$F(\mathbf{g}^{(t+1)}) \leq F(\mathbf{g}^{(t)}) + (\mathbf{g}^{(t+1)} - \mathbf{g}^{(t)})^\top \nabla F(\mathbf{g}^{(t)}) + \frac{L}{2} \|\mathbf{g}^{(t+1)} - \mathbf{g}^{(t)}\|^2. \quad (54)$$

Based on (38), the following inequality can be obtained:

$$F(\mathbf{g}^{(t+1)}) \leq F(\mathbf{g}^{(t)}) - \lambda [\nabla F(\mathbf{g}^{(t)}) - \hat{\mathbf{g}}]^\top \nabla F(\mathbf{g}^{(t)}) + \frac{\lambda^2 L}{2} \|\nabla F(\mathbf{g}^{(t)}) - \hat{\mathbf{g}}\|^2. \quad (55)$$

When $\lambda = 1/L$, the above inequality can be transformed as follows:

$$\begin{aligned} & \mathbb{E}[F(\mathbf{g}^{(t+1)})] \\ & \leq \mathbb{E} \left\{ F(\mathbf{g}^{(t)}) - \lambda [\nabla F(\mathbf{g}^{(t)}) - \hat{\mathbf{g}}]^\top \nabla F(\mathbf{g}^{(t)}) + \frac{\lambda^2 L}{2} \|\nabla F(\mathbf{g}^{(t)}) - \hat{\mathbf{g}}\|^2 \right\} \\ & = \mathbb{E} \left[F(\mathbf{g}^{(t)}) - \frac{1}{L} \|\nabla F(\mathbf{g}^{(t)})\|^2 + \frac{1}{L} (\hat{\mathbf{g}})^\top \nabla F(\mathbf{g}^{(t)}) \right. \\ & \quad \left. + \frac{1}{2L} \|\nabla F(\mathbf{g}^{(t)})\|^2 - \frac{1}{L} (\hat{\mathbf{g}})^\top \nabla F(\mathbf{g}^{(t)}) + \frac{1}{2L} \|\hat{\mathbf{g}}\|^2 \right] \\ & = \mathbb{E}[F(\mathbf{g}^{(t)})] - \frac{1}{2L} \|\nabla F(\mathbf{g}^{(t)})\|^2 + \frac{1}{2L} \mathbb{E}(\|\hat{\mathbf{g}}\|^2). \end{aligned} \quad (56)$$

By defining

$$\begin{cases} f(\mathcal{N}_t, \boldsymbol{\psi}, \mathbf{g}^{(t)}) \triangleq \sum_{n \in \mathcal{N}_t} \sum_{k=1}^K \psi_{k,n}^{(t)} \sum_{i=1}^{\beta_n} \nabla \ell(\mathbf{g}^{(t)}; \mathbf{x}_{n,i}, y_{n,i}), \\ g(\mathcal{N}_t, \boldsymbol{\psi}, \mathbf{g}^{(t)}) \triangleq \sum_{n \in \mathcal{N}_t} \sum_{k=1}^K \psi_{k,n}^{(t)} \sum_{i=1}^{\beta_n} \|\nabla \ell(\mathbf{g}^{(t)}; \mathbf{x}_{n,i}, y_{n,i})\|, \end{cases} \quad (57)$$

based on condition $S_n^{(t)} = \sum_{k=1}^K \psi_{k,n}^{(t)} = 1, \forall n \in \mathcal{N}_t$, the following inequality can be derived:

$$\begin{aligned} \mathbb{E}(\|\hat{\mathbf{g}}\|^2) & = \mathbb{E} \left[\left\| \nabla F(\mathbf{g}^{(t)}) - \frac{f(\mathcal{N}_t, \boldsymbol{\psi}, \mathbf{g}^{(t)})}{\sum_{n=1}^N S_n^{(t)} \sum_{k=1}^K \psi_{k,n}^{(t)} \beta_n} \right\|^2 \right] \\ & = \mathbb{E} \left[\left\| \frac{f(\mathcal{N}_t, \boldsymbol{\psi}, \mathbf{g}^{(t)})}{\sum_{n=1}^N \beta_n} - \frac{f(\mathcal{N}_t, \boldsymbol{\psi}, \mathbf{g}^{(t)})}{\sum_{n=1}^N S_n^{(t)} \sum_{k=1}^K \psi_{k,n}^{(t)} \beta_n} \right. \right. \\ & \quad \left. \left. + \frac{\sum_{n \in \{\mathcal{N} \setminus \mathcal{N}_t\}} \sum_{i=1}^{\beta_n} \nabla \ell(\mathbf{g}^{(t)}; \mathbf{x}_{n,i}, y_{n,i})}{\sum_{n=1}^N \beta_n} \right\|^2 \right], \end{aligned} \quad (58)$$

where $\mathcal{N} \setminus \mathcal{N}_t$ is the collection of unselected devices in round t . According to the triangle-inequality, the above inequality can be rewritten as follows:

$$\begin{aligned} \mathbb{E}(\|\hat{\mathbf{g}}\|^2) & \leq \mathbb{E} \left\{ \frac{\left[\sum_{n=1}^N \beta_n (1 - S_n^{(t)} \sum_{k=1}^K \psi_{k,n}^{(t)}) \right] g(\mathcal{N}_t, \boldsymbol{\psi}, \mathbf{g}^{(t)})}{(\sum_{n=1}^N \beta_n) (\sum_{n=1}^N S_n^{(t)} \sum_{k=1}^K \psi_{k,n}^{(t)} \beta_n)} \right. \\ & \quad \left. + \frac{\sum_{n \in \{\mathcal{N} \setminus \mathcal{N}_t\}} \sum_{i=1}^{\beta_n} \|\nabla \ell(\mathbf{g}^{(t)}; \mathbf{x}_{n,i}, y_{n,i})\|}{\sum_{n=1}^N \beta_n} \right\}^2. \end{aligned} \quad (59)$$

According to (42), inequalities

$$g(\mathcal{N}_t, \boldsymbol{\psi}, \mathbf{g}^{(t)}) \leq \sum_{n=1}^N S_n^{(t)} \sum_{k=1}^K \psi_{k,n}^{(t)} \beta_n \sqrt{\rho \|\nabla F(\mathbf{g}^{(t)})\|^2}, \quad (60)$$

and

$$\begin{aligned} & \sum_{n \in \{\mathcal{N} \setminus \mathcal{N}_t\}} \sum_{i=1}^{\beta_n} \|\nabla \ell(\mathbf{g}^{(t)}; \mathbf{x}_{n,i}, y_{n,i})\| \\ & \leq \left[\sum_{n=1}^N \beta_n \left(1 - S_n^{(t)} \sum_{k=1}^K \psi_{k,n}^{(t)} \right) \right] \sqrt{\rho \|\nabla F(\mathbf{g}^{(t)})\|^2}, \end{aligned} \quad (61)$$

can be obtained. Therefore, (59) can be rewritten as follows:

$$\begin{aligned} \mathbb{E}(\|\hat{\mathbf{g}}\|^2) & \leq \mathbb{E} \left\{ \frac{\left[\sum_{n=1}^N \beta_n \left(1 - S_n^{(t)} \sum_{k=1}^K \psi_{k,n}^{(t)} \right) \right] \sqrt{\rho \|\nabla F(\mathbf{g}^{(t)})\|^2}}{\sum_{n=1}^N \beta_n} \right. \\ & \quad \left. + \frac{\left[\sum_{n=1}^N \beta_n \left(1 - S_n^{(t)} \sum_{k=1}^K \psi_{k,n}^{(t)} \right) \right] \sqrt{\rho \|\nabla F(\mathbf{g}^{(t)})\|^2}}{\sum_{n=1}^N \beta_n} \right\}^2 \\ & = \frac{4\rho \|\nabla F(\mathbf{g}^{(t)})\|^2}{\left(\sum_{n=1}^N \beta_n \right)^2} \mathbb{E} \left[\sum_{n=1}^N \beta_n \left(1 - S_n^{(t)} \sum_{k=1}^K \psi_{k,n}^{(t)} \right) \right]^2. \end{aligned} \quad (62)$$

Due to the fact that the number of all devices' samples is not less than the number of unselected devices' samples, i.e.,

$$\sum_{n=1}^N \beta_n \geq \sum_{n=1}^N \beta_n \left(1 - S_n^{(t)} \sum_{k=1}^K \psi_{k,n}^{(t)} \right) \geq 0, \quad (63)$$

the following inequality can be obtained from (62):

$$\mathbb{E}(\|\hat{\mathbf{g}}\|^2) \leq \frac{4\rho \|\nabla F(\mathbf{g}^{(t)})\|^2}{\sum_{n=1}^N \beta_n} \mathbb{E} \left[\sum_{n=1}^N \beta_n \left(1 - S_n^{(t)} \sum_{k=1}^K \psi_{k,n}^{(t)} \right) \right]. \quad (64)$$

As a result, (56) can be rewritten as follows:

$$\begin{aligned} \mathbb{E}[F(\mathbf{g}^{(t+1)})] & \leq \mathbb{E}[F(\mathbf{g}^{(t)})] - \frac{1}{2L} \|\nabla F(\mathbf{g}^{(t)})\|^2 \\ & \quad + \frac{2\rho \|\nabla F(\mathbf{g}^{(t)})\|^2}{L \sum_{n=1}^N \beta_n} \sum_{n=1}^N \beta_n \left(1 - S_n^{(t)} \sum_{k=1}^K \psi_{k,n}^{(t)} \right). \end{aligned} \quad (65)$$

By subtracting $\mathbb{E}[F(\mathbf{g}^*)]$ in both sides of the above function, the following inequality can be obtained

$$\begin{aligned} \mathbb{E}[F(\mathbf{g}^{(t+1)}) - F(\mathbf{g}^*)] & \leq \mathbb{E}[F(\mathbf{g}^{(t)}) - F(\mathbf{g}^*)] - \frac{1}{2L} \|\nabla F(\mathbf{g}^{(t)})\|^2 \\ & \quad + \frac{2\rho \|\nabla F(\mathbf{g}^{(t)})\|^2}{L \sum_{n=1}^N \beta_n} \sum_{n=1}^N \beta_n \left(1 - S_n^{(t)} \sum_{k=1}^K \psi_{k,n}^{(t)} \right). \end{aligned} \quad (66)$$

and the proof is completed.

REFERENCES

- [1] S. Savazzi, M. Nicoli, M. Bennis, S. Kianoush, and L. Barbieri, "Opportunities of federated learning in connected, cooperative, and automated industrial systems," *IEEE Commun. Mag.*, vol. 59, no. 2, pp. 16–21, 2021.
- [2] M. Chen, D. Gündüz, K. Huang, W. Saad, M. Bennis, A. V. Feljan, and H. V. Poor, "Distributed learning in wireless networks: Recent progress and future challenges," *IEEE J. Sel. Areas Commun.*, vol. 39, no. 12, pp. 3579–3605, 2021.
- [3] Z. Qin, G. Y. Li, and H. Ye, "Federated learning and wireless communications," *IEEE Wireless Commun.*, vol. 28, no. 5, pp. 134–140, 2021.
- [4] W. Xia, W. Wen, K.-K. Wong, T. Q. Quek, J. Zhang, and H. Zhu, "Federated-learning-based client scheduling for low-latency wireless communications," *IEEE Wireless Commun.*, vol. 28, no. 2, pp. 32–38, 2021.
- [5] M. Chen, H. V. Poor, W. Saad, and S. Cui, "Wireless communications for collaborative federated learning," *IEEE Commun. Mag.*, vol. 58, no. 12, pp. 48–54, 2020.
- [6] J. Konečný, H. B. McMahan, D. Ramage, and P. Richtárik, "Federated optimization: Distributed machine learning for on-device intelligence," *arXiv preprint arXiv:1610.02527*, 2016.
- [7] S. Wang, T. Tuor, T. Salonidis, K. K. Leung, C. Makaya, T. He, and K. Chan, "Adaptive federated learning in resource constrained edge computing systems," *IEEE J. Sel. Areas Commun.*, vol. 37, no. 6, pp. 1205–1221, 2019.
- [8] M. Chen, Z. Yang, W. Saad, C. Yin, H. V. Poor, and S. Cui, "A joint learning and communications framework for federated learning over wireless networks," *IEEE Trans. Wireless Commun.*, vol. 20, no. 1, 2021.
- [9] R. Hamdi, M. Chen, A. B. Said, M. Qaraqe, and H. V. Poor, "Federated learning over energy harvesting wireless networks," *IEEE Internet Things J.*, vol. 9, no. 1, pp. 92–103, 2022.
- [10] S. Liu, G. Yu, R. Yin, J. Yuan, L. Shen, and C. Liu, "Joint model pruning and device selection for communication-efficient federated edge learning," *IEEE Trans. Commun.*, vol. 70, no. 1, pp. 231–244, 2022.
- [11] W. Shi, S. Zhou, Z. Niu, M. Jiang, and L. Geng, "Joint device scheduling and resource allocation for latency constrained wireless federated learning," *IEEE Trans. Wireless Commun.*, vol. 20, no. 1, pp. 453–467, 2021.
- [12] M. Chen, H. V. Poor, W. Saad, and S. Cui, "Convergence time optimization for federated learning over wireless networks," *IEEE Trans. Wireless Commun.*, vol. 20, no. 4, pp. 2457–2471, 2021.
- [13] T. T. Vu, D. T. Ngo, N. H. Tran, H. Q. Ngo, M. N. Dao, and R. H. Middleton, "Cell-free massive MIMO for wireless federated learning," *IEEE Trans. Wireless Commun.*, vol. 19, no. 10, pp. 6377–6392, 2020.
- [14] D. Chen, C. S. Hong, L. Wang, Y. Zha, Y. Zhang, X. Liu, and Z. Han, "Matching-theory-based low-latency scheme for multitask federated learning in mec networks," *IEEE Internet Things J.*, vol. 8, no. 14, pp. 11 415–11 426, 2021.
- [15] Z. Ji, L. Chen, N. Zhao, Y. Chen, G. Wei, and F. R. Yu, "Computation offloading for edge-assisted federated learning," *IEEE Trans. Veh. Technol.*, vol. 70, no. 9, pp. 9330–9344, 2021.
- [16] K. Wang, Z. Ding, D. K. C. So, and G. K. Karagiannidis, "Stackelberg game of energy consumption and latency in MEC systems with NOMA," *IEEE Trans. Commun.*, vol. 69, no. 4, pp. 2191–2206, 2021.
- [17] K. Wang, F. Fang, D. B. d. Costa, and Z. Ding, "Sub-channel scheduling, task assignment, and power allocation for OMA-based and NOMA-based MEC systems," *IEEE Trans. Commun.*, vol. 69, no. 4, pp. 2692–2708, 2021.
- [18] W. Dai, Y. Zhou, N. Dong, H. Zhang, and E. P. Xing, "Toward understanding the impact of staleness in distributed machine learning," *arXiv preprint arXiv:1810.03264*, 2018.
- [19] R. D. Yates, Y. Sun, D. R. Brown, S. K. Kaul, E. Modiano, and S. Ulukus, "Age of information: An introduction and survey," *IEEE J. Sel. Areas Commun.*, vol. 39, no. 5, pp. 1183–1210, 2021.
- [20] R. Talak, S. Karaman, and E. Modiano, "Improving age of information in wireless networks with perfect channel state information," *IEEE/ACM Transactions on Networking*, vol. 28, no. 4, pp. 1765–1778, 2020.
- [21] H. H. Yang, A. Arafa, T. Q. S. Quek, and H. Vincent Poor, "Age-based scheduling policy for federated learning in mobile edge networks," in *ICASSP 2020 - 2020 IEEE International Conference on Acoustics, Speech and Signal Processing (ICASSP)*, 2020, pp. 8743–8747.
- [22] J. Ren, Y. He, D. Wen, G. Yu, K. Huang, and D. Guo, "Scheduling for cellular federated edge learning with importance and channel awareness," *IEEE Trans. Wireless Commun.*, vol. 19, no. 11, pp. 7690–7703, 2020.
- [23] D. Chen, C. S. Hong, L. Wang, Y. Zha, Y. Zhang, X. Liu, and Z. Han, "Matching-theory-based low-latency scheme for multitask federated learning in MEC networks," *IEEE Internet Things J.*, vol. 8, no. 14, pp. 11 415–11 426, 2021.
- [24] Z. Yang, M. Chen, W. Saad, C. S. Hong, and M. Shikh-Bahaei, "Energy efficient federated learning over wireless communication networks," *IEEE Trans. Wireless Commun.*, vol. 20, no. 3, pp. 1935–1949, 2021.
- [25] T. Basar and G. J. Olsder, *Dynamic noncooperative game theory*. Siam, 1999, vol. 23.
- [26] Z. Han, *Game theory in wireless and communication networks: theory, models, and applications*. Cambridge University Press, 2012.
- [27] H. Tuy, "Monotonic optimization: Problems and solution approaches," *SIAM Journal on Optimization*, vol. 11, no. 2, pp. 464–494, 2000.
- [28] Y. J. A. Zhang, L. Qian, J. Huang *et al.*, "Monotonic optimization in communication and networking systems," *Foundations and Trends® in Networking*, vol. 7, no. 1, pp. 1–75, 2013.

- [29] A. Roth and M. Sotomayor, "Two-sided matching," *Handbook of game theory with economic applications*, vol. 1, pp. 485–541, 1992.
- [30] E. Bodine-Baron, C. Lee, A. Chong, B. Hassibi, and A. Wierman, "Peer effects and stability in matching markets," in *International Symposium on Algorithmic Game Theory*. Springer, 2011, pp. 117–129.
- [31] D. Ray, *A game-theoretic perspective on coalition formation*. Oxford University Press, 2007.
- [32] S. Samarakoon, M. Bennis, W. Saad, and M. Debbah, "Distributed federated learning for ultra-reliable low-latency vehicular communications," *IEEE Trans. Commun.*, vol. 68, no. 2, pp. 1146–1159, 2020.
- [33] Y. Zhao, M. Li, L. Lai, N. Suda, D. Civin, and V. Chandra, "Federated learning with non-iid data," *arXiv preprint arXiv:1806.00582*, 2018.